Journal Pre-proof

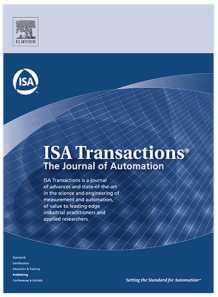

An Adaptive Predictive control scheme with dynamic Hysteresis Modulation applied to a DC-DC buck converter

Nubia Ilia Ponce de León Puig, Dimitar Bozalakov, Leonardo Acho, Lieven Vandevelde, José Rodellar

PII: S0019-0578(20)30197-X
DOI: https://doi.org/10.1016/j.isatra.2020.05.015
Reference: ISATRA 3576

To appear in: *ISA Transactions*

Received date : 13 January 2020
Revised date : 27 April 2020
Accepted date : 9 May 2020

Please cite this article as: N.I.P. de León Puig, D. Bozalakov, L. Acho et al., An Adaptive Predictive control scheme with dynamic Hysteresis Modulation applied to a DC-DC buck converter. *ISA Transactions* (2020), doi: https://doi.org/10.1016/j.isatra.2020.05.015.

An Adaptive Predictive Control Scheme with Dynamic Hysteresis Modulation Applied to a DC-DC Buck Converter

Nubia Ilia Ponce de León Puig [1], Dimitar Bozalakov [2], Leonardo Acho [3], Lieven Vandevelde [2], José Rodellar [1]

[1] Universitat Politècnica de Catalunya-UPC, BarcelonaTech.

Escola d'Enginyeria de Barcelona Est-EEBE, Department of Mathematics.

[2] Ghent University, Faculty of Engineering and Architecture, Department of Electromechanical Systems and Metal Engineering.

[3] Universitat Politècnica de Catalunya-UPC, Escola Superior d'Enginyeries Industrial, Aeroespacial i Audiovisual de Terrassa ESEIAAT.

Corresponding Author:

Nubia Ilia Ponce de León Puig

Universitat Politècnica de Catalunya-UPC, BarcelonaTech.

Escola d'Enginyeria de Barcelona Est-EEBE, Department of Mathematics

Tel: +34 615 32 50 42

E-mail: nubiliaponcepuig@gmail.com

Highlights of the submitted paper "An Adaptive Predictive Control Scheme with Dynamic Hysteresis Modulation Applied to a DC-DC Buck Converter"

- A simple adaptive-predictive control scheme for a DC-DC buck converter is proposed
- A hysteresis modulation is introduced to enrich the closed-loop control performance
- The control scheme is robust to modelling errors due to an on-line parameter estimation
- It is suited to control complex nonlinear electronic devices in renewable energy field
- Simulations and experiments in a setup verify the robustness in real cases

An Adaptive Predictive Control Scheme with Dynamic Hysteresis Modulation Applied to a DC-DC Buck Converter

Abstract

This article proposes a recent Adaptive Predictive (AP) control technique applied to a DC-DC buck converter. This converter topology has a wide range of applications in the current electronic and electrical systems that demand an efficient use of low bus voltage and specific requirements in load current consumption. Nevertheless, this converter, and in general any DC-DC converter topology, presents a control challenge due to its nonlinear nature. Hence, in this article, it is proposed an adaptive predictive control scheme that has low implementation complexity and improves the buck converter performance since it provides a fast response of the output voltage. Moreover, the output is adequately regulated even when the system is subjected to perturbations in the reference voltage, in the input voltage, in the load or in the converter parameters that may be seen as faults in the system. On the other hand, one of the main contributions of the proposed control technique with respect to other controllers is that the AP control scheme allows to on-line infer the parametric status of the plant thanks to its adaptive stage. In addition, a dynamic Hysteresis Modulator (HM) is properly inserted in the control strategy to improve the dynamic behaviour of the Adaptive Mechanism (AM), and in general, of the entire closed-loop control performance. To validate the effectiveness of the control design, a wide range of numerical experiments are carried out by using Matlab/Simulink. Finally, the developed control technique was implemented in a benchmark experimental platform. According to the experimental results, the proposed predictive control is suitable for real scenarios in the power electronics applications.

Keywords: DC-DC buck converter; adaptive predictive control; hysteresis modulation.

1. Introduction

In recent years, the power electronics field has had an enormous growth, mainly in the branch of regulation, conversion and distribution of energy [1, 2]. This, due to the high demand of electrical and electronic applications that require devices that realize these tasks. Among all the variety of power electronics devices, DC-DC converters are one of the most common and most studied by engineers and researchers [1].

Regarding to the control engineering, the DC-DC converters constitute an important challenge due to their switched nonlinear and time-varying characteristics [2, 3, 4], the fast changes in their reference voltage, their high sensitivity to the frequently changing loading conditions [5], their very small sampling period [6] and the changes in the system parameters related to external perturbations. All of these challenging tasks highly depend on the application. For instance, in photovoltaic (PV) systems, the DC-DC converter output voltage may be subjected to external perturbations due to the variations of the solar irradiation on the PV panel. These variations may be rapid, for instance, under fast shading conditions [7, 8]. Hence, the controller of the DC-DC converters applied to a PV system must be robust to changes in the input voltage and external perturbations [9]. In general, the main objective of DC-DC converters is to ensure stability with an adequate dynamic response in order to achieve a desired load output voltage by guaranteeing a good performance while optimizing the utility life of the electronic components [3]. The most common DC-DC converters are the *buck* converter, which is the one treated in this paper and basically consists in decreasing the output voltage on the load with respect to the input voltage, the *boost* converter that works to increase the voltage with respect to its input, and finally the *buck-boost* also known as *Cûk* converter, which realizes both

tasks, decreases and increases the load voltage according to the control switch position [10].

Nowadays, and because of the buck converter advantages, such as its small size, low weight, and high efficiency [2, 11, 12], it is universally used for a great amount of applications that require low bus voltage and low-to-medium load current consumption [7, 13, 14]. This converter has been employed in the realization of battery chargers [15, 16], and battery-operated portable equipment, due to its simple structure and low-cost [17, 18]. In the automotive field, the buck converter is widely used. One example of it is its bidirectional version for applications in dual battery system for hybrid electric vehicles [19, 20]. Furthermore, in the management of energy, the DC-DC converters have been adopted along with an adequate control technique, to improve the optimization of the total cost of fuel cell/battery in hybrid electric vehicles [21, 22]. Last but not least, in the renewable energies area, the buck converter also has won popularity, for instance, to feed power from distributed generators into smart grids [9] and to improve the efficiency of energy provided by photovoltaic panels through maximum power point tracking techniques [23, 24, 25].

In the last two decades, a considerable amount of control techniques have been applied to these devices, of which mainly focus on the Sliding Mode Control (SMC) technique [26, 27], which is a notable control strategy that has been applied in a wide range of engineering systems [28]. This strategy has received much attention owing to its advantages of simple structure, strong robustness and its immunity towards matched uncertainties [10, 26, 27]. However, its convergence time might be notably long and the infinite switching frequency caused by the sign function in its controller cannot be completely avoided [28]. Some improvements of the conventional SMC also have been presented with the aim of eliminating its main disadvantages, for instance, by proposing a switching sliding surface or a fixed frequency and an adaptive backstepping sliding mode control [29, 30, 31]. On the other hand, the habitual Proportional-Integral-Derivative

(PID) controller has been used in DC-DC converters because of its simplicity [4]. Nevertheless, this method does not ensure robustness over a wide range of operating points since it involves linearization around a specific operating point [4, 10]. In spite of it, PID controller has been jointly employed with other techniques to improve its performance taking advantages of the combined strategies, for instance, with a neural network based technique, with current feed-back loop by invoking hysteresis or with a finite-time control strategy [32, 33, 34]. Likewise, the Pulse-Width-Modulation (PWM) control scheme is also popular in DC-DC converters. This technique utilizes a signal modulation by reason of the switching necessity of the actuator to achieve the control objective [9, 35]. Furthermore, optimal controllers seek to solve the control problem statement by minimizing a properly designed cost function. Normally, the cost function may incorporate the uncertainties and constraints of the system which results in a proper control performance. However, the design of an adequate cost function can be a complex mathematical realization [12, 36, 37]. Other control techniques for DC-DC converters are Super-Twisting (STW) algorithms [38], Fuzzy Logic controllers [39], and Neural Networks based techniques [32, 40]. On the other hand, hysteretic controllers are an alternative way to achieve the control objective of DC-DC converters thanks to their simplicity, no need of compensation, instantaneous response and no limitations on the switch conduction time [7]. Still, the necessity of an adequate sensing stage makes that these controllers may be costly in terms of economic saving and computational work [3, 33]. Additionally, the standard Adaptive Control scheme is also an alternative to control the DC-DC converters. By using this technique, the converter not only estimates and adapts the values of the uncertain parameters but also reaches the steady state in limited time. The paper in [5] realizes a very clear summary of the adaptive techniques in the DC-DC converters state-of-art. Finally, in the area of power converters, some Predictive Control techniques have emerged as a good alternative [6, 41]. The Model Predictive Control (MPC) obtains the control action by solving an optimization problem with future prediction over a finite horizon [42]. The main advantage of this technique is that the system

constraints and nonlinearities may be considered in the cost function [6, 43]. Nevertheless, the MPC presents disadvantages, such as, the difficulty of the cost function design or the lack of stability guarantees [42, 43]. The Predictive Control technique has been successfully used in photovoltaic applications where a Maximum Power Point Tracking is combined jointly to the DC-DC converter controller to improve the efficiency of the energy provided by the photovoltaic panel [44, 45].

Since there are still many disadvantages to be defeated in the DC-DC converter controllers, this article proposes a recent control scheme for the buck converter based on an Adaptive Predictive (AP) strategy. The AP control scheme is a well established technique that has been applied in a wide variety of industrial applications [46, 47, 48]. In this article, a remodeled Adaptive Predictive control is proposed to improve the DC-DC buck converter performance. Generally speaking, the AP control strategy requires the mathematical model of the process to predict its future behaviour that is re-planed every sample time. Moreover, the AP scheme utilizes an adaptive system to auto-adjust the changes in the plant due to perturbations or faults. The strategy is established in a linear model even if the process is nonlinear, as it will be seen later in this article. This is one of the advantages of the proposed method since the control scheme is simple to conceive and implement. Besides, unlike the traditional predictive control scheme, the AP control design does not use an optimization problem and the prediction horizon is just realized one period in the future, making it a simple but effective option to reduce computational cost and to obtain a good controller performance. Additionally, an Hysteresis Modulator (HM) is inserted in the control scheme to improve the performance of the controller since it provides persistent excitation to the Adaptive Mechanism to ensure the parameters convergence [48, 49]. This extra stage in the control scheme guarantees to solve problems such as saturation in the control law and parameter drift [47], among other advantages provided by this modulation stage. Finally, it will be exposed how the Adaptive Mechanism provides on-line information about the condition

of the process parameters. This allows us to infer the status of the system, which could be useful to post-process the estimated parameters with the objective of detecting faults in the system.

In this article a wide range of experiments is presented. Firstly, numerical experiments are realized in Matlab/Simulink. Furthermore, because one of the most typical application of DC-DC converters is in the solar renewable energy field, this article presents an application of the proposed control scheme in a PV system at a numerical experiment level. This is realized by employing a PV panel as the voltage supply to the buck converter. Hence, it is validated that the proposal has a good performance even when the buck converter is subjected to the common irradiation change perturbation presented in the PV panel due to shading conditions. Secondly, the technique exposed here, is also tested in an experimental platform where the results were compared to those obtained with a typical PI controller. Hence, it will be seen that the proposed technique has a good performance since it has a fast convergence response under changes in reference voltage, in input voltage and in the load. Moreover, the controller is robust since it maintains the output voltage well regulated even when there are variations in the inductance which is one of the principal components of the converter.

Hereafter, Section 2 presents the DC-DC buck converter mathematical model. Afterward, Section 3 exposes the proposed Adaptive Predictive control. Numerical experiment results are depicted in Section 4. On the other hand, the results of the experimental implementation in a real DC-DC buck converter are shown in Section 5; the result discussion is presented in Section 6. Finally, conclusions are drawn in Section 7.

2. DC-DC Buck Converter Modeling

The conventional electronic circuit of the buck converter is shown in Fig. 1. It is mainly composed of an input voltage source (E), a switch mechanism (S), a diode (D), an inductor (L), a capacitor (C), and finally the load, which usually is a resistor (R). Based on circuit analysis and under ideal assumptions, the buck converter dynamic model may given by [10]:

$$\begin{aligned} L\dot{z}_1(t) = &\quad -z_2(t) + u(t)E, \\ C\dot{z}_2(t) = &\quad z_1(t) - \tfrac{z_2(t)}{R}, \end{aligned} \tag{1}$$

where, $z_1 = i_L$ is the inductor current, $z_2 = V_o$ is the output voltage and u is the switching control input. By assuming that the circuit is in Continuous Conduction Mode (CCM), this is, the minimum instantaneous value of the inductor current does not drop to zero even in load variation conditions, the following state normalization by using the time scale transformation $\tau = \frac{t}{\sqrt{LC}}$, may be introduced [4]:

$$x_1 = \frac{z_1}{E}\sqrt{\frac{L}{C}}, \quad x_2 = \frac{z_2}{E}. \tag{2}$$

Thus, the normalized model that will serve for control design purposes is given by [10]:

$$\begin{aligned} \dot{x}_1(t) = &\quad -x_2(t) + u(t), \\ \dot{x}_2(t) = &\quad x_1(t) - \tfrac{x_2(t)}{Q}, \\ y(t) = &\quad Ex_2(t), \end{aligned} \tag{3}$$

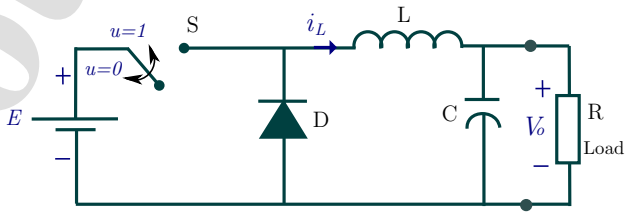

Figure 1: Buck converter electronic diagram.

where $Q = R\sqrt{C/L}$ and $y(t)$ is the output equation. Hence, $x_1(t)$ and $x_2(t)$ are now the normalized state variables, the inductor current and output voltage, respectively. From the system in equation (3) it is possible to obtain the parameterized transfer function, which will be later useful to design the Predictive Model and the Adaptive Mechanism of the control scheme. Therefore, the parameterized transfer function to (3) can be stated by its relation, in Laplace domain, between the output process $Y(s)$ and the input control $U(s)$ as folows:

$$G(s) = \frac{Y(s)}{U(s)} = \frac{a_1}{s^2 + a_2 s + a_3}, \tag{4}$$

where a_1, a_2 and a_3 are the plant parameters to be estimated by the Adaptive Mechanism, and then employed by the Predictive Model. Additionally, note that equation (4) is a second order transfer function that will facilitate to conceive the control design and it is suitable to obtain an outstanding control performance for the buck converter. This is one of the main important attributes of the proposed technique, since it is possible to control nonlinear systems through a linear control design.

3. Adaptive Predictive Control Design

In this section, the stages of the Adaptive Predictive control scheme are described. This control methodology is based on an approximated dynamic mathematical model that depicts the process to be controlled. This model is required to obtain the Predictive Model, based on a discrete-time realization, which generates the control law. On the other hand, the process model is also useful to design the Adaptive Mechanism, which serves to auto-adjust the process parameters under any possible change in the plant, provoked mainly by external perturbations or faults in the system. Figure 2 depicts the general structure of the Adaptive Predictive control [46, 47, 48]. Where, for the buck converter implementation, $y(t)$ is the converter output voltage, $y_d(k+1)$ is the desired trajectory generated by the Driver Block, $\hat{a}_1(k), \hat{a}_2(k)$ and $\hat{a}_3(k)$ are the

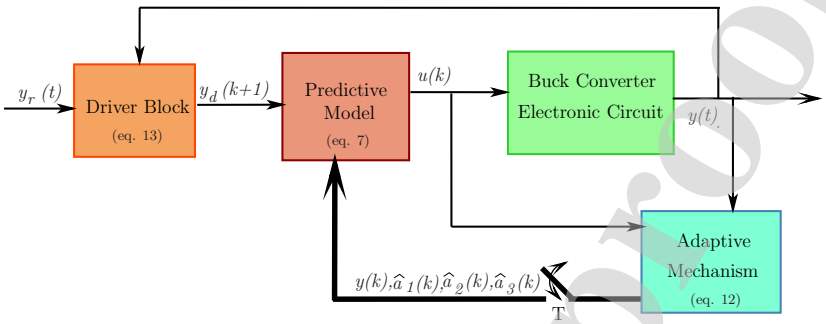

Figure 2: Adaptive Predictive control block diagram.

process estimated parameters and $u(k)$ is the control law. In addition, $y_r(t)$ is the reference voltage that may change with the time, depending on the application or the user preferences and it is processed in discrete time by the Driver Block, as well as the process output.

3.1. Predictive Model

This block generates the adaptive predictive control law $u(k)$. Since the Predictive Model is established in discrete-time domain, the Euler's discretization forward-difference law is invoked [44, 47]:

$$\frac{dx}{dt} \approx \frac{x(k+1) - x(k)}{T}, \tag{5}$$

where, T is the sampling-time period. Then, by transforming the equation (4) into discrete-time domain through the expression in (5), the Predictive Model is obtained as follows,

$$\hat{y}(k+1) = \frac{-y(k)[-\frac{2}{T^2} - \frac{\hat{a}_2(k)}{T} + \hat{a}_3(k)] - \frac{y(k-1)}{T^2} + \hat{a}_1(k)u(k)}{\frac{1}{T^2} + \frac{\hat{a}_2(k)}{T}}. \tag{6}$$

In the equation above, $\hat{y}(k+1)$ represents the prediction of the process output for the instant $k+1$ done at the instant k. Hence, the Predictive Model uses the estimated parameters by the Adaptive Mechanism at the instant k: $\hat{a}_1(k), \hat{a}_2(k)$,

$\hat{a}_3(k)$. Note that equation (6) is a future estimation of the process output that employs all the information from the dynamic process [46, 50]. Later on, the output prediction (6) is expressed as a desired value $\hat{y}(k+1) = y_d(k+1)$. This signal is perceived as a *desired trajectory projected* with its own dynamic and it is provided by the Driver Block. Thereby, the following adaptive predictive control law is obtained [46, 50, 47]:

$$u(k) = \frac{y_d(k+1)[\frac{1}{T^2} + \frac{\hat{a}_2(k)}{T}] + y(k)[-\frac{2}{T^2} - \frac{\hat{a}_2(k)}{T} + \hat{a}_3(k)] + \frac{y(k-1)}{T^2}}{\hat{a}_1(k)}. \quad (7)$$

3.2. Adaptive Mechanism

The Adaptive Mechanism (AM) design is implemented in continuous-time domain, nevertheless the estimated parameters are processed in discrete-time domain as the Predictive Model requires (see Fig. 2). The Adaptive Mechanism adjusts the model parameters to compensate the dynamic changes provoked, for instance, by external perturbations or faults in the process. Thus, the AP control scheme is robust under perturbations, since the AM stage will compensate the changes in the plant provoked by those perturbations. Due to the Adaptive Mechanism employs information from the prediction error in its model, it is not required extra mathematical or computational work to compensate the error between the output process $y(t)$ and the reference value $y_r(t)$, as other control techniques do it [6, 51].

The Adaptive Mechanism block could be seen as a "learning system", and its realization is by the well known *Gradient Algorithm* [49]. Note in Fig. 3, that the Adaptive Mechanism receives information from the process output and the control signal. In the approach presented here, the objective of this block is to obtain the parameters $\hat{a}_1, \hat{a}_2$ and $\hat{a}_3$ that are the estimation of the process parameters in (4) that accompany the process dynamic.

From the Gradient Algorithm expressed as $\dot{\hat{\theta}}(t) = -\gamma\phi(t)e(t)$, where $\gamma > 0$ is a proposed value known as *adaptation gain*, $\phi(t)$ is the regression matrix and

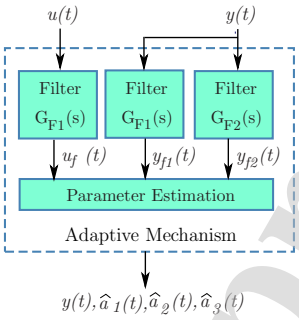

Figure 3: Adaptive Mechanism scheme.

$e(t)$ is the output estimation error $e(t) = \hat{y}(t) - y(t)$; a vector representation of the parameter estimation can be written as [49]:

$$\dot{\hat{\theta}}(t) = -\gamma\phi(t)[\hat{y}(t) - y(t)]. \tag{8}$$

The regression matrix is obtained by filtering the input and output signals of the Adaptive Mechanism (see Fig. 3). To do this, two stable second order filters are proposed:

$$G_{F1}(s) = \frac{s}{s^2 + \lambda_1 s + \lambda_2}, \quad G_{F2}(s) = \frac{1}{s^2 + \lambda_1 s + \lambda_2}, \tag{9}$$

where λ_1 and λ_2 are the design parameters of the filters. Thus, by filtering the signals and by applying basic algebra concepts, the Laplace domain process output expression is obtained:

$$Y(s) = a_1 U_f + A_2 Y_{f1} + A_3 Y_{f2} = \begin{bmatrix} a_1 & A_2 & A_3 \end{bmatrix} \begin{pmatrix} U_f \\ Y_{f1} \\ Y_{f2} \end{pmatrix} = \theta^{\star T}\phi, \tag{10}$$

where, $A_2 = \lambda_1 - a_2$, $A_3 = \lambda_2 - a_3$ and $\theta^{\star T}$ forms the parameters vector. On the other hand, U_f, Y_{f1} and Y_{f2} are the corresponding filtered signals. Then, an estimation of the equation above in continuous-time domain can be written as:

$$\hat{y}(t) = \hat{a}_1 u_f + \hat{A}_2 y_{f1} + \hat{A}_3 y_{f2} = [\hat{a}_1 \quad \hat{A}_2 \quad \hat{A}_3] \begin{pmatrix} u_f \\ y_{f1} \\ y_{f2} \end{pmatrix} = \hat{\theta}^T \phi(t), \tag{11}$$

where, $\hat{A}_2 = \lambda_1 - \hat{a}_2$ and $\hat{A}_3 = \lambda_2 - \hat{a}_3$. Finally, by replacing the equation (11) in the vector representation (8), the dynamic model that realizes the parameter estimation is obtained:

$$\begin{aligned} \dot{\hat{a}}_1 = &\quad -\gamma u_f [\hat{a}_1 u_f + \hat{A}_2 y_{f1} + \hat{A}_3 y_{f2} - y], \\ \dot{\hat{A}}_2 = &\quad -\gamma y_{f1} [\hat{a}_1 u_f + \hat{A}_2 y_{f1} + \hat{A}_3 y_{f2} - y], \\ \dot{\hat{A}}_3 = &\quad -\gamma y_{f2} [\hat{a}_1 u_f + \hat{A}_2 y_{f1} + \hat{A}_3 y_{f2} - y]. \end{aligned} \tag{12}$$

3.3. Driver Block

The aim of this block is to generate a reference trajectory to be used by the Predictive Model based on a reference model. This block basically induces that the process output smoothly evolves when the reference value or the operation point of the process variable is abruptly modified. Therefore, the Driver Block makes the task of updating at every sample time, with information from the process output $y(k)$, a desired reference trajectory $y_d(k+1)$. In this manner, the control law is physically implementable with a smooth behaviour. Hence, based on a fairly typical example of a reference model [46], in this article it is proposed the Driver Block equation as follows:

$$y_d(k+1) = \alpha_1 y_r(k) + \alpha_2 y_r(k-1) - \beta_1 y(k), \tag{13}$$

where $y_d(k+1)$ is the output signal to be employed by the Predictive Model and $y_r(k)$ is the user reference value, processed in discrete-time domain by the Driver Block. Moreover, α_1, α_2 and β_1 are the design stable parameters assigned to attenuate oscillations [52].

3.4. The Hysteresis Modulator in the Predictive Control Scheme

In the field of power electronic converters, the basic concept of hysteresis is useful, for this reason some control strategies appeal to it to accomplish its control objective [7]. This is because the actuator of the power converters is a commutator device and the hysteresis systems have a kind of on/off dynamic delay that facilitates the control implementation and improves the controller performance [53, 54]. Typically, controllers based on hysteresis consists of programming the delay band that can be fixed to a certain value or not [53]; therefore, the process output is regulated to a given reference value. For instance, the canonical behaviour of a hysteresis controller with a fixed band is represented in Fig. 4. Recently, the hysteresis controllers applied to DC-DC converters have demonstrated to be useful to adjust the system response in the event of any change of the line input voltage or load variations, to solve the problem of switching frequency variation or to avoid infinite switching frequency [3, 54, 55]. However, the techniques that appeal just to hysteresis to control the converters require more cost in sensors and the task of adequately adjust the band hysteresis may result complicated [7]. Moreover, typically, the hysteresis strategy employs a *static commutation* [7, 53, 54], it means, there is no dynamic transition in the hysteresis loop.

In this article, a *dynamic hysteresis* system is proposed as a modulator between the Adaptive Predictive control law and the plant to be controlled (see Fig. 5). This block takes advantage of the hysteresis qualities mentioned before, along with the Adaptive Predictive control scheme benefits. In this proposal, the hysteresis has an important role in the control scheme since it provides the persistent excitation required for the Adaptive Mechanism to adjust the controller dynamics [49, 56]. Moreover, the Hysteresis Modulation block acts as a modulator of the predictive control signal. In this manner, the plant receives an adequate control signal to accomplish the control objective [47]. Finally, the hysteresis provides other advantages such as avoiding saturation problems or adjusting the system response under abrupt external perturbations.

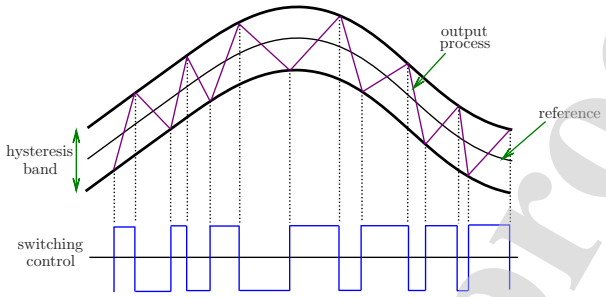

Figure 4: Performance of a fixed band hysteresis system [53].

Thereby, the predictive control scheme along with the Hysteresis Modulator is presented in Fig. 5. Moreover, the implemented dynamic hysteresis equation is proposed as follows [8, 48]:

$$\dot{z}(t) = \alpha_{hm}[-z(t) + b_{hm}\text{sgn}(x(t) + a_{hm}\text{sgn}(z(t)))], \tag{14}$$

where a_{hm} and $b_{hm} \in R^+$ are the hysteresis loop parameters and $z(t)$ is the internal variable of the hysteresis model. On the other hand, α_{hm} is the constant-transition rate. In Fig. 5, it is possible to observe that the input of the hysteresis model $x(t)$ is now the predictive control law $u(k)$ and its output will be the new control law $u_{hm}(k)$ employed by the Adaptive Mechanism and the process.

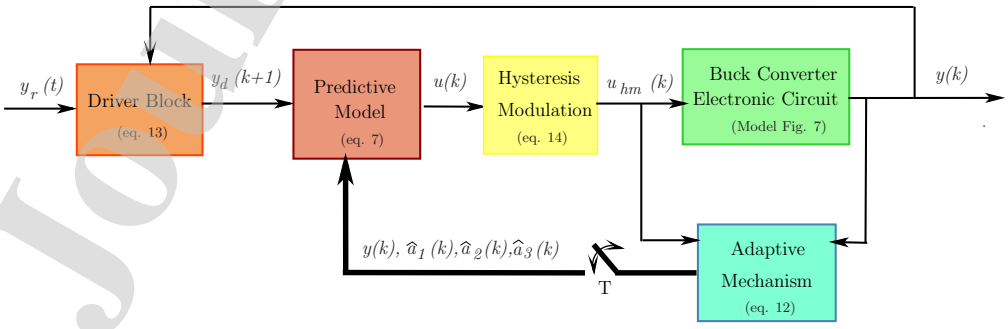

Figure 5: Scheme of the proposed control strategy along with the Hysteresis Modulation block.

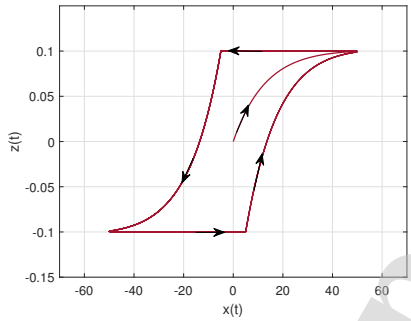

Figure 6: An hysteresis loop example.

Figure 6 is depicted as an example, to appreciate the behaviour of the hysteresis dynamic equation. This graphic is a $x(t)$ vs $z(t)$ plot of the open loop hysteresis response with parameters set as $\alpha_{hm} = 5$, $b_{hm} = 0.1$ and $a_{hm} = 5$. Furthermore, the input signal $x(t)$ is a sinusoidal one $x(t) = 50\sin(0.4\pi)$.

4. Numerical Experiment Results

In this section, different numerical experiments will be illustrated to evaluate the effectiveness of the proposed predictive control technique. These experiments were realized in Matlab/Simulink 2018b. The realistic buck converter parameters used for these simulations were obtained from a real DC-DC setup and are listed in Table 1. In addition, the parameters of the control scheme are set as follows: $\alpha_{hm} = 5$, $a_{hm} = 5$, $b_{hm} = 0.1$, $\gamma = -0.001$, $\lambda_1 = 10$, $\lambda_2 = 5$, $\alpha_1 = \alpha_2 = 100$, $\beta_1 = 200$. These parameters were tuned by the trial and error procedure by fulfilling the criteria of stability for the filters and the Driver Block equation. Finally, the sample time T is set to 0.05 ms. In Fig. 7, the Simulink model of the buck converter employed for the experiments is shown.

4.1. Step Changes in the Reference Voltage

This subsection mainly exposes how the control objective of regulating the output voltage of the buck converter is accomplished even when the reference

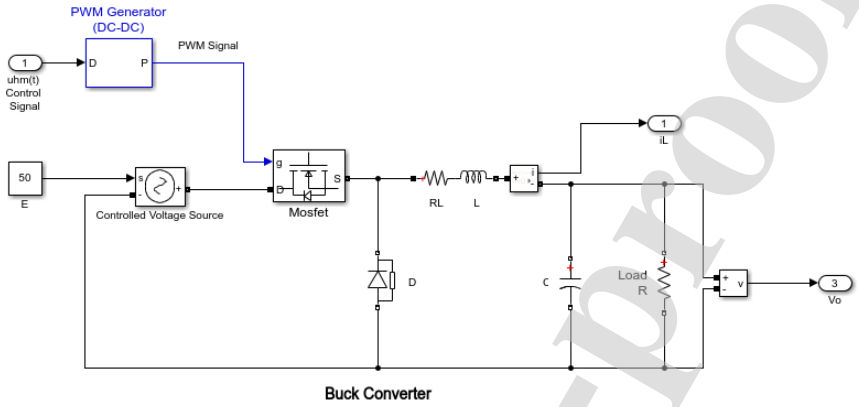

Figure 7: Buck converter Simulink model.

voltage is modified. This scenario is realistic, for instance, when the user changes the reference value according to a required application of the buck converter. In these experiments, the reference voltage is altered by step changes every second from 15 V, to 20 V, to 25 V. In Fig. 8 it is possible to observe that the control performance is satisfactorily executed since the different values of reference voltage are achieved in fast time and without overshoots. Note that the oscillation condition in the output response is due to the hysteretical nature of the closed-loop system and it does not compromise the performance of the converter controller. Moreover, depending on the application, the oscillations

Table 1: Buck converter parameters.

DC input voltage	50V
Switching frequency	20kHz
Inductor L	0.004 H
Capacitor C	2.5μ F
Load resistor R	22.2Ω
Resistor in inductor	0.04 Ω
Diode snubber resistance	0.1Ω
Diode snubber capacitance	20μ F

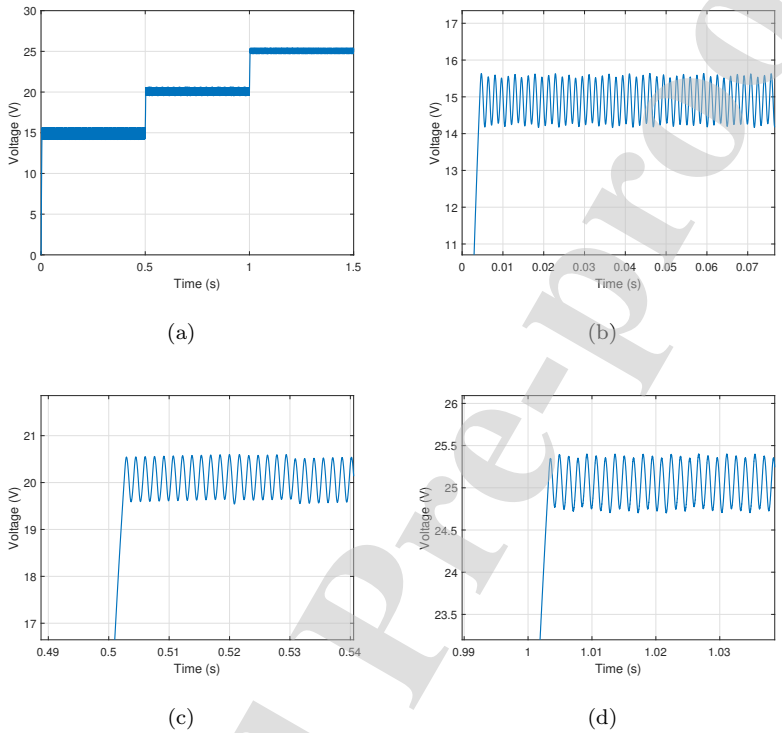

Figure 8: (a) Output voltage response with step changes in the reference voltage. (b) (c) (d) The corresponding zoom-in versions.

might be attenuated by employing adequate filters, among other techniques [57].

Finally, in order to illustrate the actuation of the control law, the PWM signal (see Fig. 7) was filtered by using a low-pass filter $G_{PWM}(s) = 10/(s+10)$. This filtered signal is shown in Fig. 9 where it is appreciable the control action every time the voltage reference is readjusted.

4.2. Step Change in the Input Voltage

In this numerical experiment, a step down change from 50 to 40 V in the input voltage occurs at 0.5 seconds. This kind of scenario is important to consider since it is a realistic situation when the voltage supply to the converter is

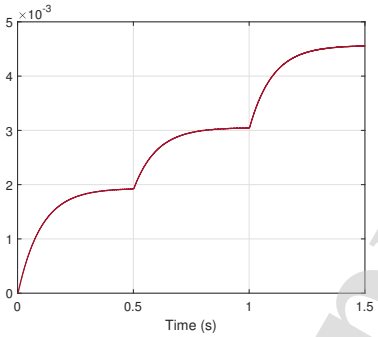

Figure 9: Filtered PWM signal.

subjected to variable voltage conditions such as voltage drop or overloading, or when the voltage supply does not have a control stage to maintain the input voltage to the converter regulated. One example of this scenario could be a DC-DC power converter used in a photovoltaic system. The result of this experiment is shown in Fig. 10. From this, it is possible to observe that the needed time to reach the reference voltage (20 V) is approximately 5 milliseconds. Moreover, when the input voltage changes from 50 V to 40 V at 0.5 seconds, the system takes approximately the same time to retrieve the voltage reference value.

4.3. Step Change in the Load Resistance

This subsection presents the numerical experiment results with a step change in the converter load. Just as the previous experiments, the variation in the load is also a realistic case in DC-DC converters applications. For instance, when an inductive motor linked to the DC-DC converter is broken down, the load seen by the converter will vary from its original value. This is why, this experiment is also useful to validate the proposed control technique. In this simulation, the change in the load is invoked at 0.5 seconds, from 22.2Ω to 27.2Ω, and the reference voltage is 25 V. Additionally, it is shown the response of the process estimated parameters $\hat{a}_1$, $\hat{a}_2$ and $\hat{a}_3$. This is useful to observe two important keys of the Adaptive Mechanism: 1) the dynamic response of the parameters,

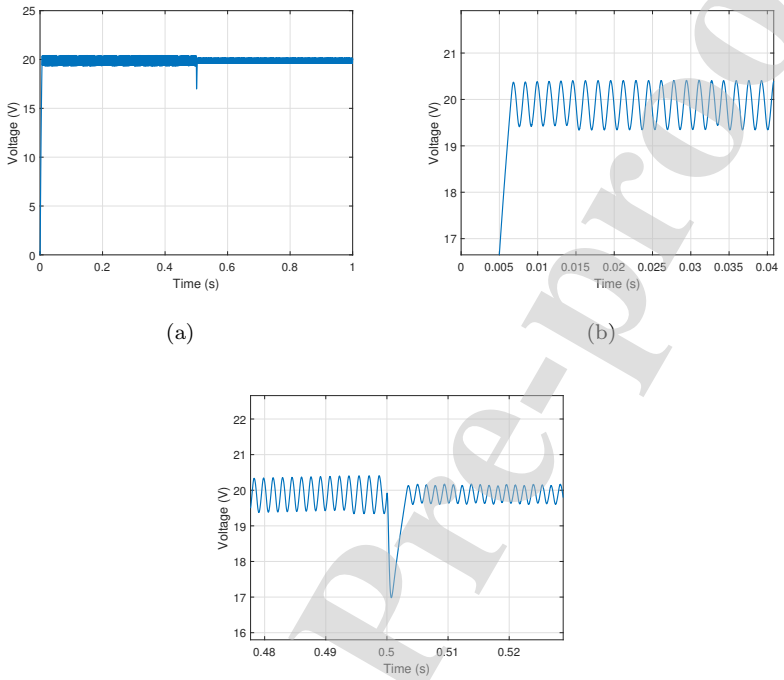

Figure 10: (a) Output voltage response with a step down change in the input voltage. (b) (c) The corresponding zoom-in versions.

and 2) the utility of this block of giving information about the parameters variation to infer when an abrupt change occurs in the process. In this experiment, the value of the gain $\gamma = -1000$ is greater than in the previous simulations to accelerate the dynamic of the adaptive system since it is slower than the control scheme dynamic [58]. The process output response is presented in Fig. 11. On the other hand, the estimated parameters are depicted in Fig. 12 where it is possible to note the variation in the estimated parameters $\hat{a}_2$ and $\hat{a}_3$ when the change in the load is invoked.

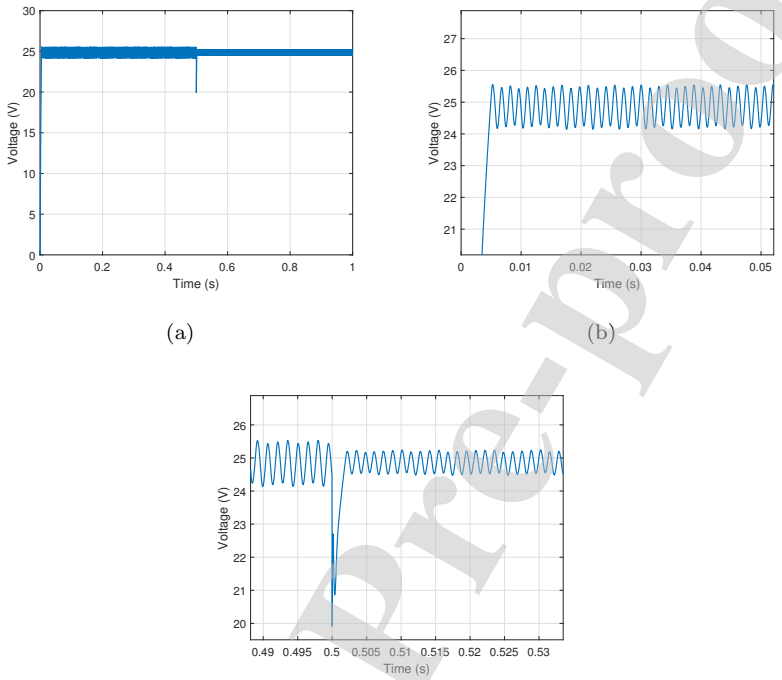

Figure 11: (a) Output voltage response with a step up change in the load. (b) (c) The zoom-in versions.

4.4. Step Change in the Inductor Parameter

For this numerical analysis, a fault in the inductance L was introduced at 0.5 seconds. This fault was simulated by abruptly change the value of the inductance from 0.002 H to 0.004 H. The reference value is 25 V. Figure 13 exposes the output voltage response. Additionally, in this experiment it is also shown the estimated parameters behaviour in Fig. 14, where it is observable the parameters reaction when the fault in the inductor occurs.

4.5. The Control Strategy Applied to a Buck Converter in Photovoltaic System

One of the most important current application of DC-DC converters is in the field of renewable energies. Therefore, in this subsection a numerical experiment

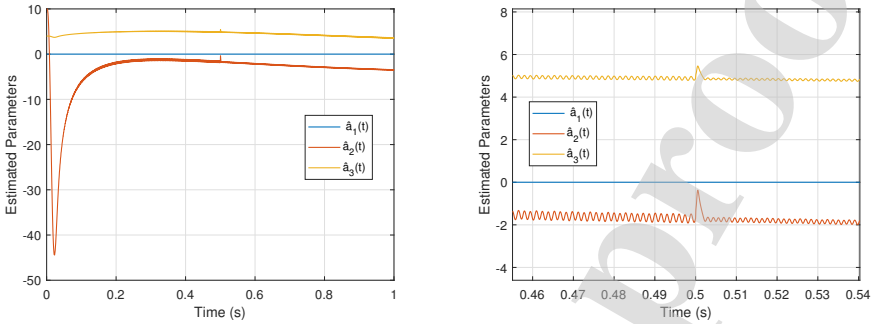

(a) (b)

Figure 12: (a) Estimated parameters when a step change load occurs at 0.5 seconds. (b) The corresponding zoom-in graphic.

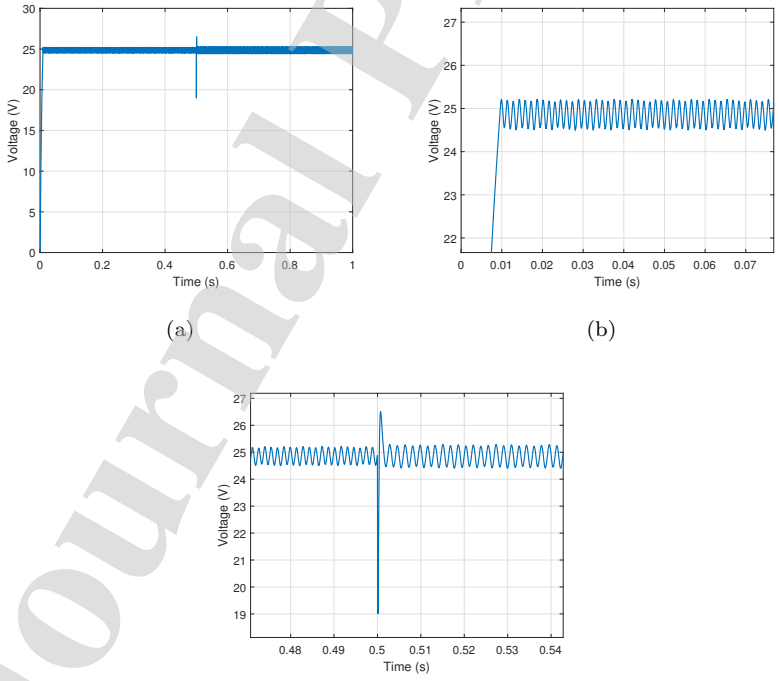

(a) (b)

(c)

Figure 13: (a) Output voltage response with a step change in the inductor. (b) (c) The corresponding zoom-in graphics.

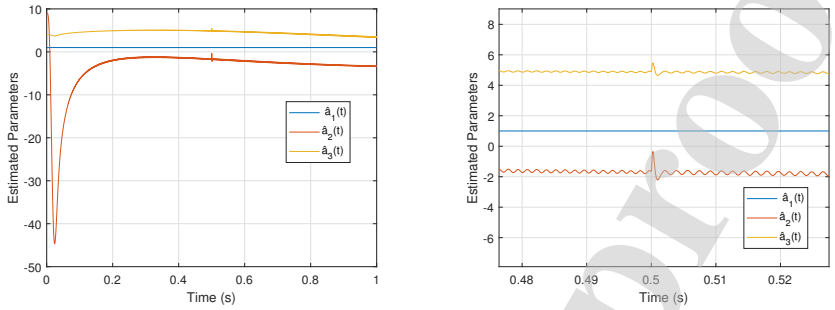

(a) (b)

Figure 14: (a) Estimated parameters with an induced error in the inductance value. (b) The zoom-in graphic.

by using a PV system is presented. In this experiment, the input voltage of the DC-DC buck converter is provided by a photovoltaic panel as is shown in Fig. 15. The implemented PV array was the SunPower SPR serie 305-E, included in the libary Simscape in Simulink. This array consists on strings of 66 PV modules connected in parallel. Each string consists of 5 modules connected in series. For this experiment, the condition of temperature was fixed at 28° C and the irradiance seen by the PV panel was modeled as shown in Fig. 16. This was programmed with changes that may emulate shading conditions. The reference voltage was fixed at 90 V and the parameters of both the control scheme and the buck converter, are the same used in the previous exposed numerical experiments. Fig. 17 shows the input voltage of the converter provided by the PV panel under the changes in the irradiance. On the other hand, Fig. 18 shows the converter output voltage where it is worth to notice that the reference value is achieved even under the different values of the irradiance in the PV panel.

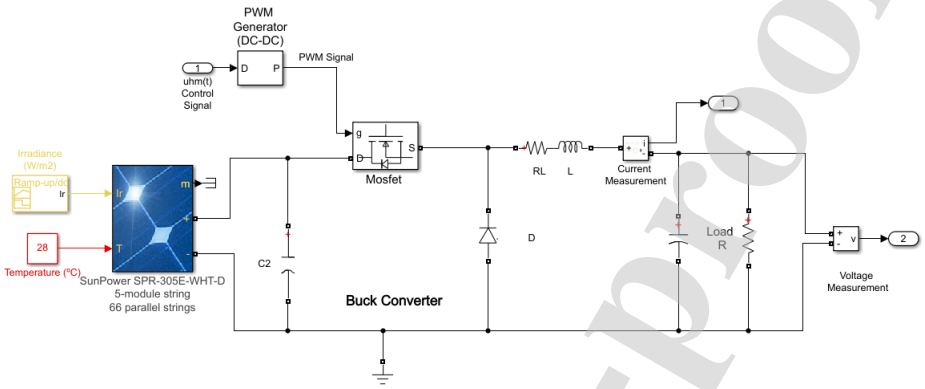

Figure 15: Buck converter implementation in Simulink by employing a PV panel array as the voltage supply.

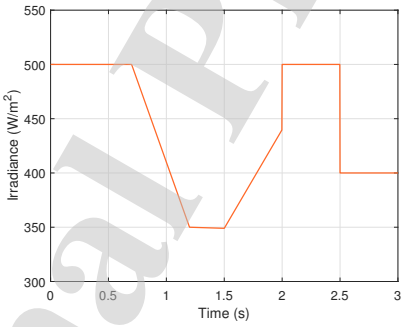

Figure 16: Different levels of irradiance.

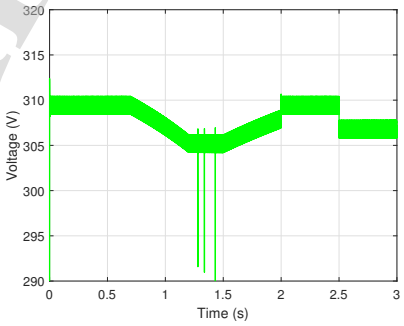

Figure 17: Supplied voltage from the PV panel.

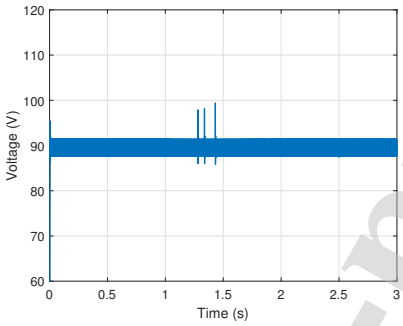

Figure 18: Output voltage with supplied voltage from the PV panel.

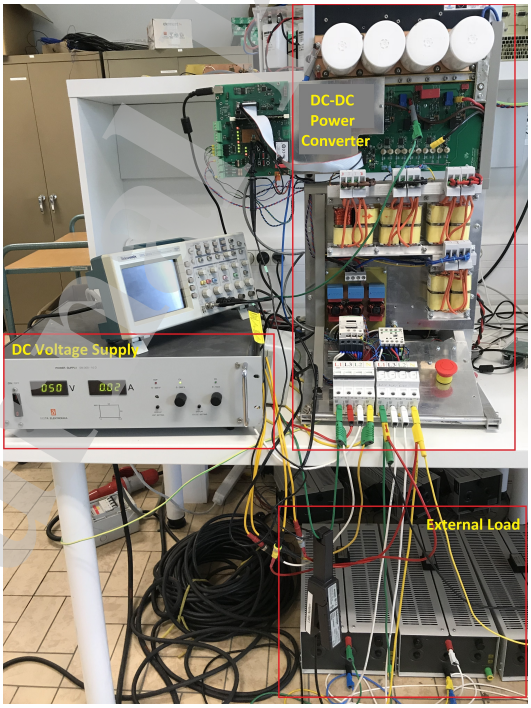

Figure 19: Experimental platform.

5. Results of the Control Implementation in a Realistic Buck Converter Setup

In order to experimentally validate the proposed predictive control, a variety of experiments were carried out using a benchmark platform in the Electrical Energy Laboratory (EELAB) in Ghent University. The parameters of each component are listed in Table 1. Furthermore, the setup is the one presented in Fig. 19, which is a three-phase inverter described in [59, 60]. However, it was adjusted such that only one leg is used to get a buck converter configuration where the proposed control algorithm was implemented. The setup is integrated with a DSP Texas Instrument processor, model TMS320F28335. This processor provides a clock speed of 150 MHz and a floating-point unit.

The results obtained with the proposed technique are compared with the results obtained by employing a common PI controller. The parameters of the PI controller are $k_i = 0.999$ rad/s^2 and $k_p = 0.001$ rad/s. Worth mentioning, that for the experimental implementation, the Adaptive Mechanism stage was not programmed, instead of it, constant values were employed to program the predictive control in equation (7). This is possible since, if the dynamic of the Adaptive Mechanism is slow (due to a small value of γ), the estimated parameters can be conceived as constant values and under an ideal assumption, they are the nearest possible to the nominal process parameters. Then, for the experiments, the estimated parameters are set $\hat{a}_1 = 0.1$, $\hat{a}_2 = 4$ and $\hat{a}_3 = 10$. On the other hand, the values for the AP control scheme are $\alpha_{hm} = 8$, $b_{hm} = 5$, $\alpha_1 = \alpha_2 = 10$ and $\beta_1 = 20$.

5.1. Change in the Reference Voltage

In Fig. 20 the response of the output voltage (Ch1: yellow signal) is depicted when the reference voltage of the buck converter has a step change from 0 V to 20 V. The time per division in Fig. 20(a) is 500 microseconds, on the other

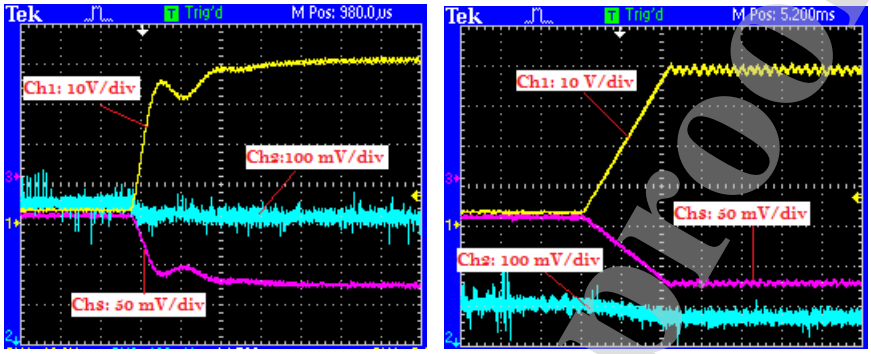

(a) (b)

Figure 20: Output voltage response (Ch1), load current (Ch2) and inductor current (Ch3), under a step up change in the reference voltage from 0 V to 20 V by employing PI controller (a) and the proposed AP controller (b).

hand, in Fig. 20(b) is 5 milliseconds. From here, it is notable that the time that takes the output voltage in achieving the stable reference value in both cases, the PI controller and the proposal AP control, is similar. However, the response with the proposed control technique is better than the one with the PI controller since it does not present overshoots. A similar conclusion can be deduced from the experiment when the reference voltage has a step change from 20 V to 0 V in Fig. 21. Here the time per division is 1 millisecond and 10 milliseconds, respectively. Signals blue (Ch2) and magenta (Ch3) are the measured current through the load and in the inductor converter, respectively. Note that in these experiments the voltage probe was scaled by two the original measured value.

5.2. Step Change in the Input Voltage

The results presented in this subsection were obtained by inducing a step change in the input voltage from 50 V to 100 V and vice versa. The reference value was set at 25 V. Fig. 22 gathers the results when the input voltage has a step up change. On the other hand, Fig. 23 recovers the results when the input voltage varies from 100 V to 50 V. In both cases, by employing both control

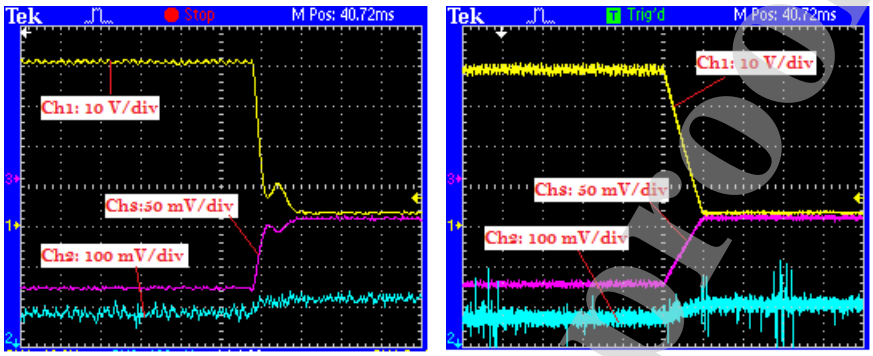

(a) (b)

Figure 21: Output voltage response (Ch1), load current (Ch2) and inductor current (Ch3), under a step down change in the reference voltage from 20 V to 0 V by employing PI controller (a) and the proposed AP controller (b).

techniques, the results are very similar. The system barely notes the change and it maintains the output voltage (Ch1) in the desired value. In these experiments the time per division is 25 milliseconds. Additionally, the green signal (Ch4) is the input voltage to the buck converter and the magenta signal (Ch3) is the converter current. Finally, the blue signal (Ch2) shows the moment when the change in the input voltage occurs. From Fig. 23, the measured inductor current shows that there is a spike with a high di/dt. Thus, it is worth to mention that this transient does not result into a change of the output voltage and it is presented in both control algorithms, it may be concluded that the origin of this issue is in the measurement system and not due to malfunction in the controllers.

5.3. Step Change in the Load

In this experiment, a step change in the load is induced from 22.2 Ω to 27.2Ω and vice versa. First, when the step up change is invoked, the time per division in the results with the PI control technique is 1 millisecond and 100 microseconds in the zoom version. On the other hand, the time per division for the results with the AP proposal, is 5 milliseconds and 2.5 milliseconds in the

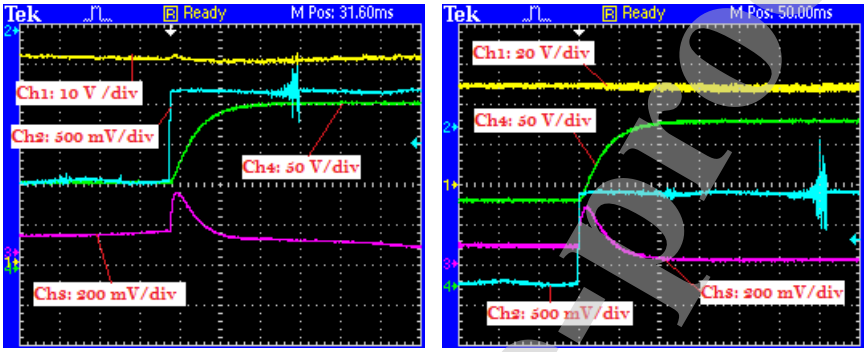

(a) (b)

Figure 22: Output voltage response (Ch1), current inductor (Ch3) and input voltage (Ch4), under a step up change in the input voltage from 50 V to 100 V by employing PI controller (a) and the proposed AP controller (b).

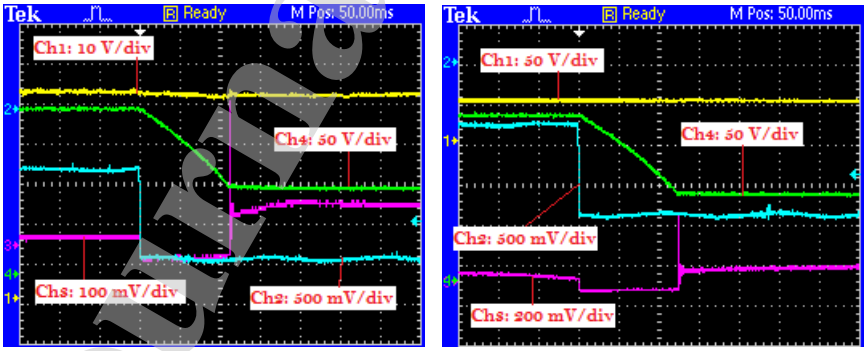

(a) (b)

Figure 23: Output voltage response (Ch1), current inductor (Ch3) and input voltage (Ch4), under a step down change in the input voltage from 100 V to 50 V by employing PI controller (a) and the proposed AP controller (b).

zoom version. From Fig. 24, it is visible that the time in achieving the reference voltage value is a bit faster with the PI controller, nevertheless in contrast with it, the response of the AP controller does not present the overshoot unlike the case with the PI control. In this figure, the green signal (Ch4) is used to identify when the change in the load occurs. The set of graphics in Fig. 25 presents alike results obtained by doing the step down change in the load. In these results, the time per division for the PI case is 2.5 milliseconds and 250 microseconds in the zoom versions. Moreover, the time per division for the AP case is 5 milliseconds and 1 millisecond in the zoom version.

5.4. Step Change in the Inductor

The set of graphics in Fig. 26 depicts the experiment results when a step up change in the inductor is triggered from 2mH to 4mH. Although this scenario may not be present in practice, since an abrupt change in the inductor may mean the converter is completely broken down, it is a good experiment to validate robustness of the control technique. This experiment was realized by switching the corresponding transistor in the setup to make the adequate array with the inductors. In this specific experiment, the AP control has a faster response (5 milliseconds/div and 1 millisecond/div in the zoom version) than the PI case (2.5 milliseconds/div and 55 microseconds/div in the zoom version). Moreover, the PI controller results contain more overshooting. In these experiments, the green signal (Ch4) represents the exact moment when the inductors are switching. On the other hand, Fig. 27 depicts the results by doing the step down change in the inductor. Note that in this case, for both controllers, the system barely notices the change. Here, the time per division is 250 microseconds and 2.5 milliseconds, respectively.

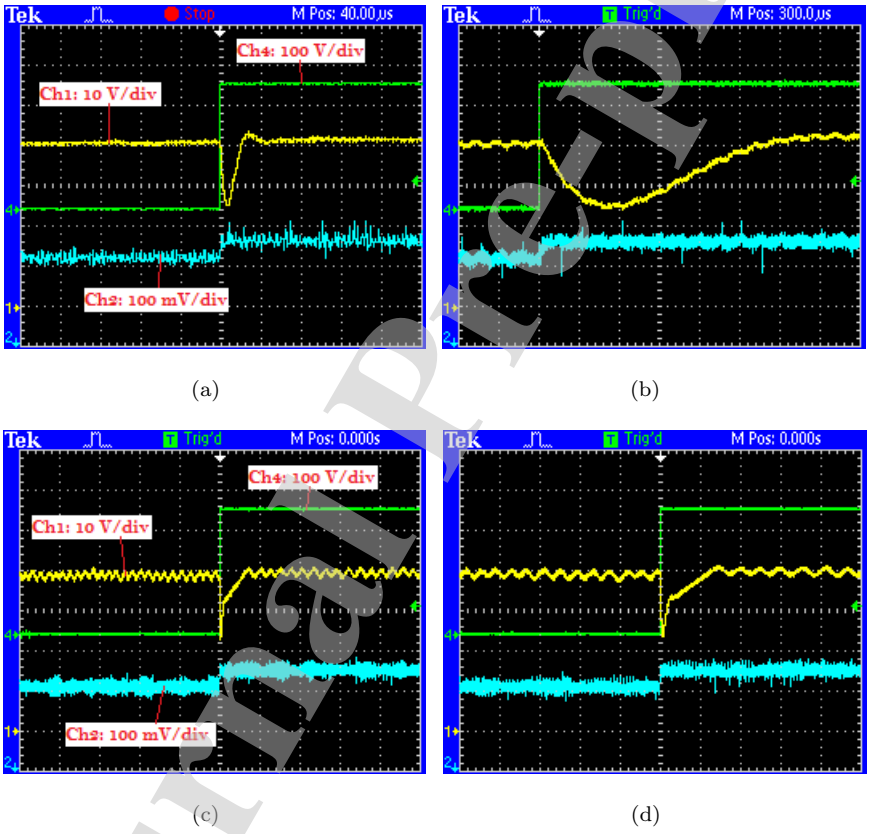

Figure 24: Output voltage response (Ch1), and inductor current (Ch2) under a step up change in the load from 22.2Ω to 25.2Ω by employing PI controller (a) and its zoom version (b), and the proposed AP controller (c) and its zoom version (d).

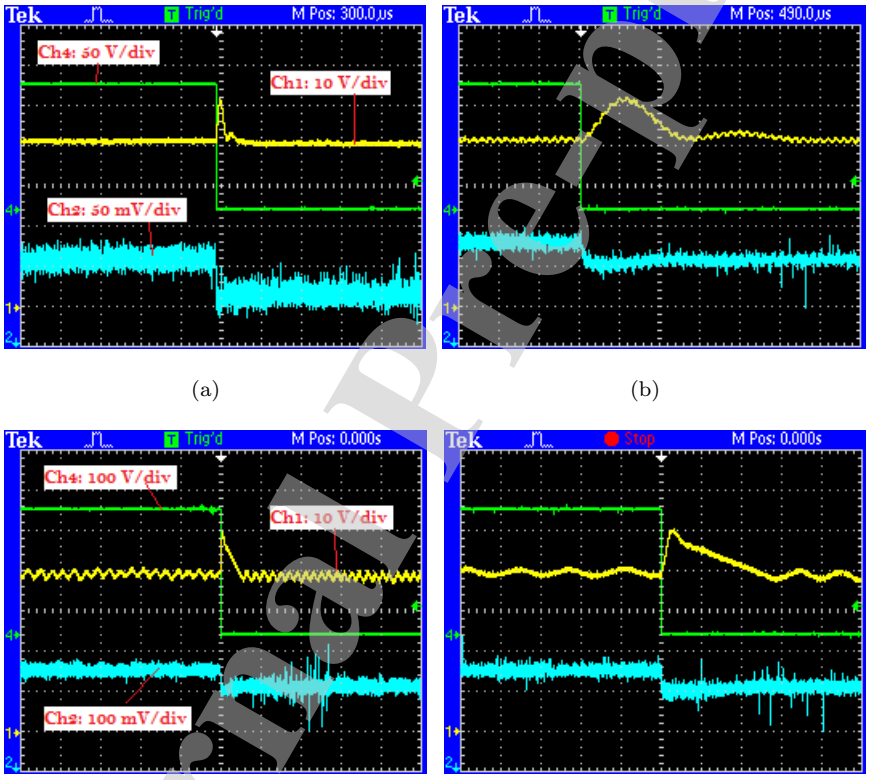

Figure 25: Output voltage response (Ch1), and inductor current (Ch2) under a step down change in the load from 25.2Ω to 22.2Ω by employing PI controller (a) and its zoom version (b), and the proposed AP controller (c) and its zoom version (d).

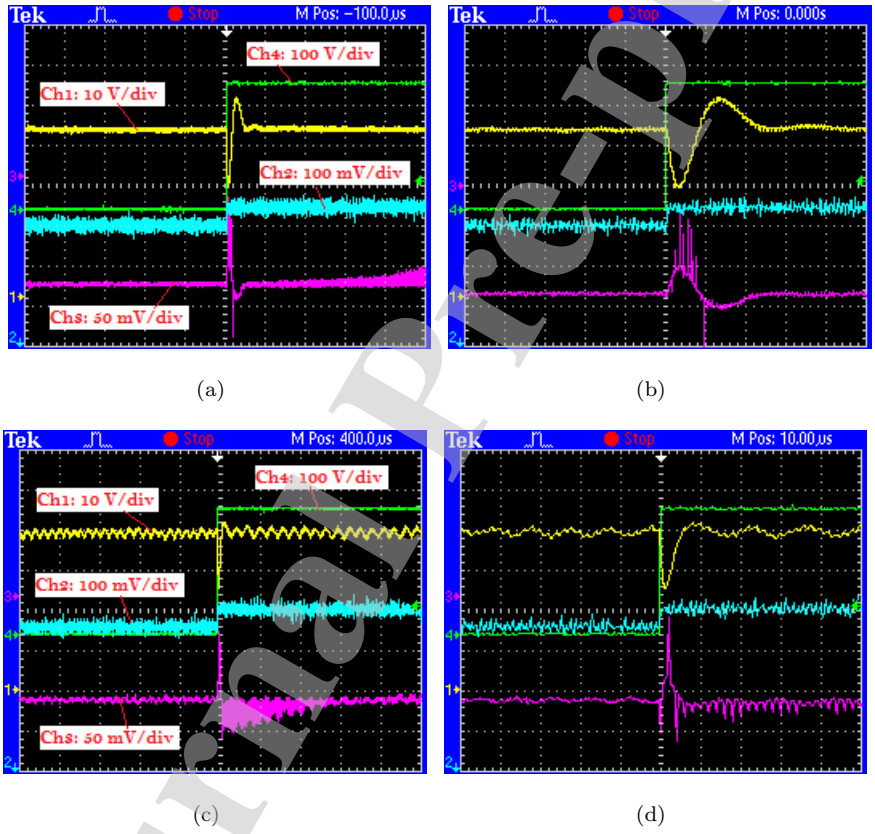

Figure 26: Output voltage response (Ch1), inductor current (Ch2), and load current (Ch3) under a step up change in the inductor from 2 mH to 4 mH by employing PI controller (a) and its zoom version (b), and the proposed AP controller (c) and its zoom version (d).

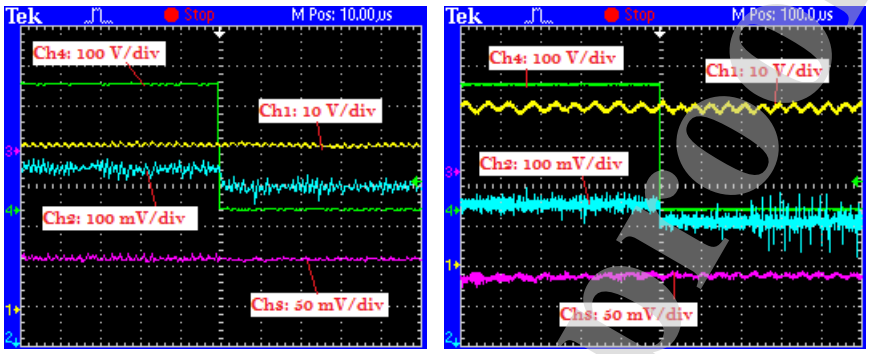

(a) (b)

Figure 27: Output voltage response (Ch1), inductor current (Ch2), and load current (Ch3) under a step down change in the inductor from 4 mH to 2 mH by employing PI controller (a) and its zoom version (b), and the proposed AP controller (c) and its zoom version (d).

6. Discussion of Results

In this article, the presented results, both numerical and experimental, allow us to draw some conclusions regarding the proposed control technique. Firstly, the results make inference that the Adaptive Predictive control strategy is an adequate option to control the buck converter device since its main objective is totally accomplished. That is, regulate the output voltage to a desired value. Realistic scenarios have been emulated in numerical simulations and experimental implementation and in all cases the control strategy works as expected. If a comparison between the results from numerical experiments and real implementation is made, it can be seen that the time response is slower in the real cases. This difference is mainly because the simulation model uses ideal conditions, while in the case of the real implementation, the system is subjected to different conditions, for instance, the signal-processing time, the velocity of the controller processing unit and the optimal useful life of the actuators, among other characteristics always presented in real control systems. Nevertheless, even in the real implementation, the proposed technique provides acceptable results in the time response and in the robustness of the controller. On the other hand, as was presented in Section 5, the conventional PI controller is a good option to accom-

plish the objective, however this kind of controller has a limited behaviour when the system is subjected to external perturbations, for instance when the value of the inductor varies (Fig. 26). As it was shown in the experimental results, the AP control technique works better than the case with the PI controller when the parameters of the system are subjected to changes, external perturbations or faults. For this reason, in general, the exposed proposal can be considered as a better option since the AP control technique is more robust than the PI controller. On the other hand, the proposal allows to extract more information from the system thanks to the parameter estimation phase. Hence, the objective in a near future is to implement the stage of the Adaptive Mechanism in the setup in order to diagnose the system in real time. Nonetheless, from numerical experiments it is possible to deduce since now, that this phase will work as expected. Finally, from numerical and experimental results, it is notable that the output voltage contains a ripple characteristic. This is an essential condition produced by the hysteresis modulation stage and it is typically presented in controllers with hysteresis. Normally, the DC-DC converter objective is about regulation, and since the plant itself or the user load may behave as signal filters, this rippling behaviour is usually accepted in most of the implementation scenarios. In comparison with other control strategies in the state-of-the-art, the main contribution of this paper lies in the on-line process state monitoring by the hystereticaly manipulated adaptive mechanism. Additionally, this adaptive stage is also able to compensate possible mismatched errors in the process modeling during the control design. Thus, the proposed control approach does not require an accurate mathematical model of the process to obtain the control law, unlike, for instance, the conventional predictive control design. Finally, the low complexity of the control technique makes possible to reduce mathematical and computational efforts in comparison, for instance, to the conventional optimal control techniques.

7. Conclusions

In this paper, a new control scheme for a DC-DC buck converter has been completely developed and tested through numerical and real experiments. The control approach is a simple manner to accomplish the main power control objective of these electronic devices. That is, efficiently regulating the output voltage of a DC-DC converter to a desired value even when the system is subjected to the commonly existing perturbations, such as variation in the input voltage, fast changing in the reference command voltage, or a possible fault in some of the buck-process parameters. The proposed predictive control scheme has been experimentally evaluated in a benchmark platform outcoming to be robust under different faulty scenarios. Moreover, the exposed results, both numerical and experimental, show that the control objective is quickly accomplished, which is a notable and always required property in the field of DC-DC converter applications. On the other hand, the theoretical and analytical outcomes exhibited in this article about an adaptive predictive control design are the basis of a planned future work, where it is expected to implement the proposed control scheme into a whole distributed energy system where the main energy is supplied by a renewable source. Hence, the predictive control strategy will have to accomplish the control objective of extracting the maximum power from a renewable source even when it is subjected to external perturbations, efficiently regulating the extracted voltage through a DC-DC converter; and properly controlling a DC-AC inverter coupled to a grid network.

Acknowledgments

This work has been partially funded by the Spanish Ministry of Economy and Competitiveness/Fondos Europeos de Desarrollo Regional (MINECO/FEDER) with grant number DPI2015-64170-R and by the scholarship for doctoral studies abroad provided by the CONACyT, Mexico.

References

[1] N. Mohan, T. M. Undeland, Power electronics: converters, applications, and design, John wiley & sons, 2007.

[2] A. Kislovski, Dynamic analysis of switching-mode DC/DC converters, Springer Science & Business Media, 2012.

[3] H. Komurcugil, Non-singular terminal sliding-mode control of DC-DC buck converters, Control Engineering Practice 21 (3) (2013) 321–332.

[4] H. Sira-Ramirez, Nonlinear PI controller design for switchmode DC-to-DC power converters, IEEE Transactions on Circuits and Systems 38 (4) (1991) 410–417.

[5] T. K. Nizami, C. Mahanta, An intelligent adaptive control of DC-DC buck converters, Journal of the Franklin Institute 353 (12) (2016) 2588–2613.

[6] Z. Leng, Q. Liu, A simple model predictive control for buck converter operating in CCM, in: 2017 IEEE International Symposium on Predictive Control of Electrical Drives and Power Electronics (PRECEDE), IEEE, 2017, pp. 19–24.

[7] M. Castilla, L. G. de Vicuna, J. M. Guerrero, J. Miret, N. Berbel, Simple low-cost hysteretic controller for single-phase synchronous buck converters, IEEE transactions on Power Electronics 22 (4) (2007) 1232–1241.

[8] N. Ponce de León Puig, L. Acho, J. Rodellar, Design and experimental implementation of a hysteresis algorithm to optimize the maximum power point extracted from a photovoltaic system, Energies 11 (7) (2018) 1866.

[9] Z. Wang, S. Li, J. Yang, Q. Li, Current sensorless finite-time control for buck converters with time-varying disturbances, Control Engineering Practice 77 (2018) 127–137.

[10] H. Sira-Ramírez, On the generalized PI sliding mode control of DC-to-DC power converters: a tutorial, International journal of control 76 (9-10) (2003) 1018–1033.

[11] K. E. L. Marcillo, D. A. P. Guingla, E. M. Rocha, W. Barra, D. A. V. Benavides, R. L. P. de Medeiros, Parameter optimization of an interval robust controller of a buck converter subject to parametric uncertainties, in: 2018 IEEE Third Ecuador Technical Chapters Meeting (ETCM), IEEE, 2018.

[12] Z. Leng, J. Liu, Q. Liu, H. Wang, A digital optimal control method for DC-DC converters based on simple model, in: 2008 workshop on Power Electronics and intelligent Transportation System, IEEE, 2008, pp. 88–93.

[13] G. Singh, V. Verma, S. Urooj, A. Haque, Regulation of DC bus voltage for DC microgrid using psim, in: 2018 5th IEEE Uttar Pradesh Section International Conference on Electrical, Electronics and Computer Engineering (UPCON), IEEE, 2018.

[14] H. Wang, W. Wu, Y. Li, F. Blaabjerg, A coupled-inductor-based buck-boost AC-DC converter with balanced dc output voltages, IEEE Transactions on Power Electronics 34 (1) (2018) 151–159.

[15] W. Li, Y. Zheng, W. Li, X. He, et al., A smart and simple PV charger for portable applications, in: 2010 Twenty-Fifth Annual IEEE Applied Power Electronics Conference and Exposition (APEC), IEEE, 2010, pp. 2080–2084.

[16] B. Liu, R. Ren, F. Wang, D. Costinett, Z. Zhang, A variable frequency zvs control of a three-level buck without zero crossing detection for wide-range output voltage battery chargers, in: 2019 IEEE Applied Power Electronics Conference and Exposition (APEC), IEEE, 2019, pp. 2311–2316.

[17] R.-J. Wai, R.-Y. Duan, High-efficiency power conversion for low power fuel

cell generation system, IEEE Transactions on Power Electronics 20 (4) (2005) 847–856.

[18] C. Gavriluta, C. Citro, K. Nisak, H. B. San Segundo, A simple approach for fast controller prototyping for a three phase interleaved DC-DC converter, in: 2012 IEEE International Symposium on Industrial Electronics, IEEE, 2012, pp. 2015–2019.

[19] O. García, P. Zumel, A. De Castro, A. Cobos, Automotive DC-DC bidirectional converter made with many interleaved buck stages, IEEE Transactions on Power Electronics 21 (3) (2006) 578–586.

[20] D. C. Erb, O. C. Onar, A. Khaligh, Bi-directional charging topologies for plug-in hybrid electric vehicles, in: 2010 Twenty-Fifth Annual IEEE Applied Power Electronics Conference and Exposition (APEC), IEEE, 2010, pp. 2066–2072.

[21] X. Hu, C. Zou, X. Tang, T. Liu, L. Hu, Cost-optimal energy management of hybrid electric vehicles using fuel cell/battery health-aware predictive control, IEEE Transactions on Power Electronics 35 (1) (2019) 382–392.

[22] X. Hu, Y. Li, C. Lv, Y. Liu, Optimal energy management and sizing of a dual motor-driven electric powertrain, IEEE Transactions on Power Electronics 34 (8) (2018) 7489–7501.

[23] Y. Jiang, J. A. A. Qahouq, T. A. Haskew, Adaptive step size with adaptive-perturbation-frequency digital MPPT controller for a single-sensor photovoltaic solar system, IEEE transactions on power Electronics 28 (7) (2013) 3195–3205.

[24] Q. Li, P. Wolfs, A review of the single phase photovoltaic module integrated converter topologies with three different DC link configurations, IEEE Transactions on Power Electronics 23 (3) (2008) 1320–1333.

[25] A. Dehghanzadeh, G. Farahani, H. Vahedi, K. Al-Haddad, Model predictive control design for DC-DC converters applied to a photovoltaic system,

International Journal of Electrical Power & Energy Systems 103 (2018) 537–544.

[26] Y. M. Alsmadi, V. Utkin, M. A. Haj-ahmed, L. Xu, Sliding mode control of power converters: DC/DC converters, International Journal of Control 91 (11) (2018) 2472–2493.

[27] C. Edwards, S. Spurgeon, Sliding mode control: theory and applications, Crc Press, 1998.

[28] V. Utkin, Sliding mode control of DC/DC converters, Journal of the Franklin Institute 350 (8) (2013) 2146–2165.

[29] G. Ma, B. Wang, D. Xu, L. Zhang, Switching control strategy based on non-singular terminal sliding mode for buck converter in auxiliary energy source, Energy Procedia 145 (2018) 139–144.

[30] D. B. W. Abeywardana, B. Hredzak, V. G. Agelidis, A fixed-frequency sliding mode controller for a boost-inverter-based battery-supercapacitor hybrid energy storage system, IEEE Transactions on Power Electronics 32 (1) (2017) 668–680.

[31] F. Liping, Y. Yazhou, K. Boshnakov, Adaptive backstepping based terminal sliding mode control for DC-DC converter, in: 2010 International Conference on Computer Application and System Modeling (ICCASM 2010), Vol. 9, IEEE, 2010.

[32] H. Maruta, H. Taniguchi, F. Kurokawa, A study on effects of different control period of neural network based reference modified PID control for DC-DC converters, in: 2016 15th IEEE International Conference on Machine Learning and Applications (ICMLA), IEEE, 2016, pp. 460–465.

[33] C. H. Rivetta, A. Emadi, G. A. Williamson, R. Jayabalan, B. Fahimi, Analysis and control of a buck DC-DC converter operating with constant power load in sea and undersea vehicles, IEEE Transactions on Industry Applications 42 (2) (2006) 559–572.

[34] C. Yuan, Y. Huangfu, R. Ma, B. Zhao, H. Bai, Nonlinear PI and finite-time control for dc-dc converter based on exact feedback linearization, in: IECON 2019-45th Annual Conference of the IEEE Industrial Electronics Society, Vol. 1, IEEE, 2019, pp. 6398–6403.

[35] S. Oucheriah, L. Guo, PWM-based adaptive sliding-mode control for boost DC-DC converters, IEEE Transactions on Industrial Electronics 60 (8) (2013) 3291–3294.

[36] A. N. Vargas, L. P. Sampaio, L. Acho, L. Zhang, J. B. do Val, Optimal control of DC-DC buck converter via linear systems with inaccessible markovian jumping modes, IEEE Transactions on Control Systems Technology 24 (5) (2016) 1820–1827.

[37] K. Sundareswaran, K. Kuruvinashetti, B. Hariprasad, P. Sankar, P. Nayak, V. Vigneshkumar, Optimization of dual input buck converter control through genetic algorithm, IFAC Proceedings Volumes 47 (1) (2014) 142–146.

[38] A. Chalanga, S. Kamal, L. M. Fridman, B. Bandyopadhyay, J. A. Moreno, Implementation of super-twisting control: Super-twisting and higher order sliding-mode observer-based approaches, IEEE Transactions on Industrial Electronics 63 (6) (2016) 3677–3685.

[39] P. Siano, C. Citro, Designing fuzzy logic controllers for DC-DC converters using multi-objective particle swarm optimization, Electric Power Systems Research 112 (2014) 74–83.

[40] M. Jafari, Z. Malekjamshidi, Design, simulation and implementation of an adaptive controller on base of artificial neural networks for a resonant DC-DC converter, in: 2011 IEEE Ninth International Conference on Power Electronics and Drive Systems, IEEE, 2011, pp. 1043–1046.

[41] G. Zhou, J. Xu, Y. Jin, Improved digital peak current predictive control for switching DC-DC converters, IET Power Electronics 4 (2) (2011) 227–234.

[42] R. P. Aguilera, D. E. Quevedo, Predictive control of power converters: Designs with guaranteed performance, IEEE Transactions on Industrial Informatics 11 (1) (2015) 53–63.

[43] J. B. Rawlings, D. Q. Mayne, Model predictive control: Theory and design, Nob Hill Pub. Madison, Wisconsin, 2009.

[44] A. Lashab, D. Sera, J. M. Guerrero, A dual-discrete model predictive control-based mppt for pv systems, IEEE Transactions on Power Electronics 34 (10) (2019).

[45] Y. Shan, J. Hu, Z. Li, J. M. Guerrero, A model predictive control for renewable energy based AC microgrids without any PID regulators, IEEE Transactions on Power Electronics 33 (11) (2018) 9122–9126.

[46] J. M. Sánchez, J. Rodellar, ADEX Optimized adaptive controllers and systems, Springer, 2015.

[47] N. I. Ponce de León Puig, L. Acho Zuppa, J. Rodellar Benedé, Adaptive predictive control of a base-isolated hysteretic system, in: ICSTCC 2017: 21st International Conference on System Theory, Control and Computing: Sinaia, Romania: October 19-21, 2017: proceedings book, 2017, pp. 395–400.

[48] N. I. P. de León Puig, L. Acho, J. Rodellar, Y. Vidal, J. E. M. Gutíerrez-Arias, Hysteretic delta modulator to prevent parameter drift in adaptive-based controllers, in: 2017 25th Mediterranean Conference on Control and Automation (MED), IEEE, 2017, pp. 48–53.

[49] S. Sastry, M. Bodson, Adaptive Control: Stability, Convergence and Robustness, Courier Corporation, 1989.

[50] J. M. Sánchez, J. Rodellar, Adaptive Predictive Control: From the Concepts to Plant Optimization, Prentice Hall PTR, 1995.

[51] B. Wang, G. Ma, D. Xu, L. Zhang, J. Zhou, Switching sliding-mode control strategy based on multi-type restrictive condition for voltage control of buck converter in auxiliary energy source, Applied energy 228 (2018) 1373–1384.

[52] K. Ogata, Y. Yang, Modern control engineering, Vol. 4, London, 2002.

[53] T. Nguyen-Van, R. Abe, K. Tanaka, A digital hysteresis current control for half-bridge inverters with constrained switching frequency, Energies 10 (10) (2017) 1610.

[54] Q. Yao, D. G. Holmes, A simple, novel method for variable-hysteresis-band current control of a three phase inverter with constant switching frequency, in: Conference Record of the 1993 IEEE Industry Applications Conference Twenty-Eighth IAS Annual Meeting, IEEE, 1993, pp. 1122–1129.

[55] S.-C. Tan, Y. Lai, C. K. Tse, M. K. Cheung, Adaptive feedforward and feedback control schemes for sliding mode controlled power converters, IEEE Transactions on Power Electronics 21 (1) (2006) 182–192.

[56] C.-C. Fuh, H.-H. Tsai, Adaptive parameter identification of servo control systems with noise and high-frequency uncertainties, Mechanical systems and signal Processing 21 (3) (2007) 1437–1451.

[57] M. Rashid, Power electronics: Circuits, devices and applications (international edition), Prentice Hall, Erscheinungsdatum (2003).

[58] K. J. Åström, B. Wittenmark, Adaptive control, Courier Corporation, 2013.

[59] D. V. Bozalakov, M. J. Mnati, J. Laveyne, A. Van den Bossche, L. Vandevelde, Voltage unbalance and overvoltage mitigation by using the three-phase damping control strategy in battery storage applications, in: 2018 7th International Conference on Renewable Energy Research and Applications (ICRERA), IEEE, 2018, pp. 753–759.

[60] D. Bozalakov, M. J. Mnati, J. Laveyne, J. Desmet, L. Vandevelde, Battery storage integration in voltage unbalance and overvoltage mitigation control strategies and its impact on the power quality, Energies 12 (8) (2019) 1501.

Highlights of the submitted paper "An Adaptive Predictive Control Scheme with Dynamic Hysteresis Modulation Applied to a DC-DC Buck Converter"

- A simple adaptive-predictive control scheme for a DC-DC buck converter is proposed
- A hysteresis modulation is introduced to enrich the closed-loop control performance
- The control scheme is robust to modelling errors due to an on-line parameter estimation
- It is suited to control complex nonlinear electronic devices in renewable energy field
- Simulations and experiments in a setup verify the robustness in real cases

Declaration of interests

☒ The authors declare that they have no known competing financial interests or personal relationships that could have appeared to influence the work reported in this paper.

☐The authors declare the following financial interests/personal relationships which may be considered as potential competing interests: